Application of Modified Rod Drop Technique for Shut-Off Rod Worth Measurement in HANARO Using Time-Dependent Monte Carlo Simulations

Jae Woo Lee a, Dong Hyuk Lee b and Hyung Jin Shim a*

^aDepartment of Nuclear Engineering, Seoul National University, 1 Gwankak-ro, Gwanak-gu, Seoul, Korea ^bKorea Atomic Energy Research Institute, 111 Daedeok-daero 989 beon-gil, Yuseong-gu, Daejeon, Korea *Corresponding author: shimhj@snu.ac.kr

*Keywords: reactivity measurement, modified rod drop technique, McCARD/G code, HANARO, the Exact PKE

1. Introduction

Reactivity measurement is one of the most fundamental techniques in reactor physics, for core design and reactor control. Among reactivity measurement, accurate derivation of reactivity worth, such as control rod worth, plays a crucial role in both research reactors and power reactors. Traditionally, rod drop experiments have been widely used for rod worth measurement.

In the conventional one-point reactor kinetics model, the flux distribution is assumed to remain constant during the measurement. However, this assumption may introduce significant uncertainties, especially when measuring large reactivity worth, such as in rod drop experiments, because the flux shape is in fact time-dependent.

To overcome these limitations, recent studies [1,2] have introduced space-time kinetics models based on the exact point dynamics, explicitly accounting for the time-dependent flux shape function. Through such efforts, it has becomes possible to reduce the uncertainty associated with detector position and to achieve consistent reactivity values across different detectors.

In this study, a modified rod drop method [1] is applied to the HANARO reactor in order to evaluate reactivity worth. In the experiments, two or three SORs(Shut-Off Rods) were dropped, and the reactivity was measured using three ex-core detectors. The measured detector signals were further corrected to obtain the refined reactivity values.

2. Methods

2.1 HANARO Reactor

The HANARO research reactor is an open-tank-in pool type facility designed for various purposes such as the production of cold neutrons, irradiation experiments, and others. Uranium silicide fuel with 19.75wt% [3] enrichment is used, heavy water (D_2O) serves as a reflector, and light water (H_2O) is used as a coolant [4].

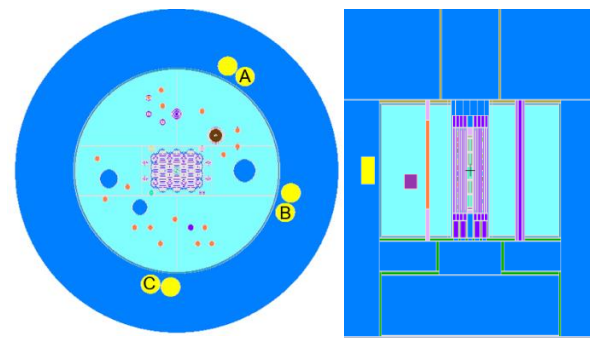


Fig. 1. Radial and Axial View of HANARO reactor with ex-core detectors

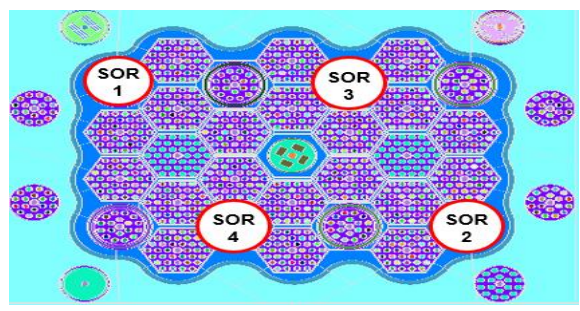


Fig. 2. Top view of inner core with SOR positions

The SORs consist of four hafnium neutron absorbers with an inner diameter of 67mm, an outer diameter of 76mm, and a length of 700mm. Zircaloy tubes are welded to both the upper and lower ends of the rods. These rods regulate neutron absorption by moving vertically along the outer surface of the cylindrical flow tubes within the reactor core. During normal operation, the SORs are positioned above the fuel assemblies, while in emergency shutdowns they are rapidly dropped into the core. In addition, three ex-core detectors are installed on the outer wall of the reflector tank, and their locations are shown in Fig. 1.

2.2 Computational Code: McCARD/G

McCARD [5] is a Monte Carlo neutron transport code developed at Seoul National University. Its time-dependent Monte Carlo (TDMC) capability is essential for transient analysis, but is computationally demanding on CPUs. To address this, a GPU-enhanced version, McCARD/G [6] was developed, providing significant speedup while retaining accuracy. In this study,

McCARD/G was employed to perform the TDMC calculations for reactivity worth analysis.

2.3 Conventional rod drop experimental technique

In the one-point reactor model, the neutron flux $\Phi(r, E, \Omega, t)$ is factorized into a amplitude function p(t) and a shape function $\psi(r, E, \Omega)$.

$$\Phi(\mathbf{r}, E, \mathbf{\Omega}, t) = p(t)\psi(\mathbf{r}, E, \mathbf{\Omega}). \tag{1}$$

Based on this factorization, several reactivity evaluation formulas can be derived from the Point Kinetics Equations (PKEs), such as the Extrapolation method, the Inverse method, and the Integral Counting method, as shown in the following [7-9]:

$$\rho = \frac{n_1 - n_0}{n_1} \beta_{eff},\tag{2}$$

$$\rho = \beta_{eff} + \Lambda \frac{d}{dt} [\ln n(t)]$$

$$-\beta_{eff} \int_{0}^{\infty} \sum_{i=1}^{6} \frac{\lambda_{i} \beta_{i}}{\beta} e^{-\lambda_{i} \tau} \frac{n(t-\tau)}{n(t)} d\tau, \qquad (3)$$

$$\rho = \frac{n_0}{\int_0^\infty n(t)dt} \sum_{i=1}^6 \frac{\beta_{i,eff}}{\lambda_i},\tag{4}$$

where ρ is the dynamic reactivity, n_1 is the detector signal immediately after the rod drop, n_0 is the detector signal before the rod drop, β_{eff} is the effective fraction of delayed neutron, Λ is the neutron generation time, n(t) is the neutron density, λ is the delayed neutron decay constant. The ENDF/B-VII.1 cross-section libraries were used in this study. Since $\psi(r, E, \Omega)$ is assumed to be unchanged in the conventional one-point model, neutron detector signal n(t) is assumed to be proportional to the amplitude function p(t). Therefore, n(t) is replaced by p(t) in Eq. (2)-(4). However, since the shape function is time-dependent and changes greatly during the measurement, the assumption that p(t) can reaplee n(t) is violated which may lead to inaccuracies.

2.3 Detector signal correction [1]

According to the Exact Point Dynamics [10], the neutron flux $\Phi(r, E, \Omega, t)$ can be factorized into a time-dependent amplitude function p(t), and a space-, energy-, angular-, and time-dependent shape function $\psi(r, E, \Omega, t)$.

$$\Phi(\mathbf{r}, \mathbf{E}, \mathbf{\Omega}, \mathbf{t}) = p(t)\psi(\mathbf{r}, \mathbf{E}, \mathbf{\Omega}, \mathbf{t}). \tag{5}$$

p(t) can be extracted as follows:

$$= \frac{N_{Det}(t)}{\int_{V} \int_{0}^{\infty} \int_{4\pi} W(\boldsymbol{r}, E, \boldsymbol{\Omega}) \psi(\boldsymbol{r}, E, \boldsymbol{\Omega}, t) d\boldsymbol{r} dE d\boldsymbol{\Omega}},$$
 (6) where $W(\boldsymbol{r}, E, \boldsymbol{\Omega})$ is the neutron detector response

where $W(\mathbf{r}, E, \mathbf{\Omega})$ is the neutron detector response function as a weight function, $N_{Det}(t)$ is the neutron signal at detector position. To avoid the calculation of $W(\mathbf{r}, E, \mathbf{\Omega})$ which may introduce an inaccuracy, normalization about the p(t) is performed as follows:

$$\overline{p(t)} = \frac{N_{Det}(t)}{N_{Det}(0)} \cdot \frac{\psi(r_d, 0)}{\psi(r_d, t)}.$$
 (7)

 $\psi(r_d, t)$ is the shape function at the detector position. By substituting the normalized $\overline{p(t)}$ into Eq. (2)-(4) instead of n(t), the dynamic reactivity ρ_{dyn} can be obtained.

2.4 Shape function at detector position $\psi(\mathbf{r_d}, t)$ [1,10]

By constraining the shape function, which leads to shift of the major time dependence into the amplitude function, $\psi(r_d, t)$ can be described as

$$= \frac{\psi(\mathbf{r}_{d}, t)}{\int_{V} \int_{0}^{\infty} \int_{4\pi} \frac{\phi_{0}^{\dagger}(\mathbf{r}, E, \mathbf{\Omega}) \phi(\mathbf{r}, E, \mathbf{\Omega}, t)}{v(E)} d\mathbf{r} dE d\mathbf{\Omega}}.$$
 (8)

 $\phi(r_d, t)$ is the detector neutron flux, $\phi_0^{\dagger}(r, E, \Omega)$ is the initial adjoint flux, v(E) is the neutron velocity. In this study, the denominator on the right side of Eq. (8) is substituted into the total flux of the core $\Phi_{total}(t)$.

$$\Phi_{total}(t) = \int_{V} \int_{0}^{\infty} \int_{4\pi} \phi(\mathbf{r}, E, \mathbf{\Omega}, t) d\mathbf{r} dE d\mathbf{\Omega}. \quad (9)$$

Therefore, the normalized amplitude function, $\overline{p(t)}$ is finally applied as follows:

$$\overline{p(t)} = \frac{N_{Det}(t)}{N_{Det}(0)} \cdot \frac{\frac{\phi(r_d, 0)}{\Phi_{total}(0)}}{\frac{\phi(r_d, t)}{\Phi_{total}(t)}}.$$
 (10)

3. Application

In order to apply the modified rod drop technique to the HANARO reactor, shut-off rod(SOR) drop experiments were carried out under controlled conditions. During the experiments, the control absorber rods(CARs) were kept at fixed positions, while the SORs were initially fully withdrawn and then released. Each SOR fell by approximately 70cm into the core, providing a strong negative reactivity insertion within a short time.

Two representative cases were considered: Case 1, in which SOR 2, 3, and 4 were dropped simultaneously, and Case 2, in which SOR 3 and 4 were dropped. During the transients, the neutron number density and neutron flux

were evaluated for both the three ex-core detectors and the entire core.

For the measurement, both static and dynamic calculations were required and the procedure was as follows:

- (1) Perform eigenvalue calculations twice, before and after the rod drop, to obtain the static k_{eff} values and calculate static reactivity, ρ_{st} .
- (2) Perform a time-dependent Monte Carlo(TDMC) calculation to obtain the neutron number density and flux at the detector position, $\phi(r_d, t)$ and throughout the entire core, $\Phi_{total}(t)$ over time. Derive $\overline{p(t)}$ and obtain the measured dynamic reactivity, ρ_{dyn} .

3.1 Static Reactivity, ρ_{st} calculation

The static reactivity was calculated using the McCARD/G eigenvalue calculation with 1,000,000 neutron histories for 1,000 active cycles after 100 inactive cycles. Eigenvalue calculations were performed twice: once before and once after the SOR drop.

$$\rho_{st} [pcm] = \left(\frac{1}{k_{eff}^{after}} - \frac{1}{k_{eff}^{before}}\right) * 10^5.$$
 (11)

 k_{eff}^{after} is the calculated k_{eff} after the SOR drop, and k_{eff}^{beore} is that before the drop.

3.2 Dynamic Reactivity, ρ_{dyn} calculation

$$\overline{p(t)} = \frac{N_{Det}(t)}{N_{Det}(0)} \cdot \frac{\phi(r_d, 0)}{\phi(r_d, t)} \cdot \frac{\Phi_{total}(t)}{\Phi_{total}(0)}.$$
 (12)

McCARD/G TDMC calculation was performed with 10,000 batches, each containing 1,000,000 neutrons and 1,000,000 precursors with 0.1ms time interval. The number of fission source convergence steps and precursor generation steps were set to be 50 and 100 steps respectively.

The normalized amplitude function $\overline{p(t)}$, was obtained from the detector number density, the neutron flux at the detector position, and the total flux at the core calculated by the TDMC calculation. This $\overline{p(t)}$ replaced n(t) in Eqs. (2)-(4) to evaluate the dynamic reactivity, ρ_{dyn} .

In addition, during the McCARD/G TDMC calculation, the kinetics parameter tally function [11] was used to obtain the kinetics parameters, and the values at the steady state just before the rod drop were applied in this study.

Table I: Kinetics parameter obtained in Case 1

Group	$\lambda_i [s^{-1}] (SD)$	$\beta_{i,eff}$ (SD)								
1	$0.01333 (1.32 \times 10^{-9})$	$0.00024 (7.96 \times 10^{-6})$								
2	$0.03272 (6.3 \times 10^{-9})$	$0.00123 (2.16 \times 10^{-5})$								
3	$0.1208 (1.15 \times 10^{-8})$	$0.00124 (1.89 \times 10^{-5})$								
4	$0.30294 (9.39 \times 10^{-8})$	$0.00275 (3.48 \times 10^{-5})$								
5	$0.84993 (2.53 \times 10^{-7})$	$0.00115 (1.7 \times 10^{-5})$								
6	$2.85451 (8.78 \times 10^{-7})$	$0.00048 (1.01 \times 10^{-5})$								
β_{eff}	$0.00711 (7.54 \times 10^{-5})$									
$\Lambda[s]$	$0.00008 (1.23 \times 10^{-7})$									

Table II: Kinetics parameter obtained in Case 2

Group	$\lambda_i [s^{-1}]$ (SD)	$\beta_{i,eff}$ (SD)							
1	$0.01333 (4.54 \times 10^{-9})$	$0.00027 (1.26 \times 10^{-5})$							
2	$0.03272 (2.17 \times 10^{-8})$	$0.00128 (3.66 \times 10^{-5})$							
3	$0.1208 (4 \times 10^{-8})$	$0.00124 (3.18 \times 10^{-5})$							
4	$0.30294 (3.24 \times 10^{-7})$	$0.0028 (5.87 \times 10^{-5})$							
5	$0.84993 (8.7 \times 10^{-7})$	$0.00116 (3.07 \times 10^{-5})$							
6	$2.85451 (3.03 \times 10^{-6})$	$0.0005 (1.82 \times 10^{-5})$							
β_{eff}	$0.00728 (1.18 \times 10^{-4})$								
$\Lambda[s]$	$0.00008 (1.74 \times 10^{-7})$								

4. Results

In the result section, reactivity measurements were evaluated under two conditions: Case 1 and Case 2. For each case, two categories of dynamic reactivity values were obtained: $\rho_{dyn,r}$, directly from the measured number density without any correction, and $\rho_{dyn,c}$, from the normalized amplitude function, $\overline{p(t)}$. In both approaches, the Extrapolation method, the Inverse method, and the Integral Counting method were applied to extract the dynamic reactivity values. Also the static reactivity, ρ_{st} was obtained from eigenvalue calculations. The R.Diff values in the tables represent the relative differences between the dynamic reactivity results and the reference static reactivity.

4.1 Case 1: Dropping SOR 2, 3 and 4

In this case, the values of $\rho_{dyn,r}$ were obtained from 7 independent runs, each with a different random number generator seed, while $\rho_{dyn,c}$ was obtained from a single run.

 $\rho_{dyn,r}$ shows noticeable deviations from the ρ_{st} regardless of the large number of neutron histories. In particular, the Extrapolation and Inverse method yield relatively large differences, indicating that neglecting the correction for the shape function introduces inaccuracies in reactivity estimation.

On the other hand, $\rho_{dyn,c}$ obtained using the normalized amplitude function $\overline{p(t)}$, demonstrates much better agreement with the static reactivity. Across all three methods – Extrapolation, Inverse, and Integral Counting- the differences between $\rho_{dyn,c}$ and ρ_{st} are considerably reduced compared to those of $\rho_{dyn,r}$.

Position	E		on metho	od	Inverse method (SD) [pcm]				Integral Counting method (SD) [pcm]				$ ho_{st}$
			(t) Raw l		Data $\overline{p(t)}$		Raw Data		$\overline{p(t)}$		(SD)		
	$\rho_{dyn,r}$	R.Diff	$ ho_{dyn,c}$	R.Diff	$\rho_{dyn,r}$	R.Diff	$ ho_{dyn,c}$	R.Diff	$\rho_{dyn,r}$	R.Diff	$\rho_{dyn,c}$	R.Diff	[pcm]
Det A	12118 (245)	+20%	11623 (123)	+15%	12122 (66)	+20%	11117 (69)	+10%	10779 (51)	+6%	10017 (119)	-0.6%	
Det B	14638 (304)	+45%	11576 (122)	+14%	14454 (84)	+43%	11084 (71)	+9%	12845 (61)	+27%	9980 (118)	-1%	10087 (4)
Det C	13430 (281)	+33%	11133 (118)	+10%	13141 (76)	+30%	10995 (73)	+9%	11539 (55)	+14%	9880 (117)	-2%	

Table Ⅲ. Reactivity obtained by dropping SOR 2, 3 and 4 (Case 1)

Table IV: Reactivity obtained by dropping SOR 3 and 4 (Case 2)

	E	vtranolati	ion metho	vd	Inverse method				Integral Counting method				
Position	E.		[pcm]	ď	(SD) [pcm]				(SD) [pcm]				$ ho_{st}$
	` ´ j¹ -		\overline{p}	<u>t)</u>	Raw	Raw Data		$\overline{p(t)}$		Raw Data		$\overline{p(t)}$	
	$\rho_{dyn,r}$	R.Diff	$\rho_{dyn,c}$	R.Diff	$\rho_{dyn,r}$	R.Diff	$\rho_{dyn,c}$	R.Diff	$\rho_{dyn,r}$	R.Diff	$\rho_{dyn,c}$	R.Diff	[pcm]
Det A	9373	+24%	8523	+12%	8977	+18%	8368	+10%	8046	+6%	7490	-0.7%	7546
	(559)		(138)	T12/0	(135)		(84)		(154)		(138)		
Det B	6878	6878 -8%	8203	+8%	7548	+0.1%	8306	+10%	6691	-11%	7457	-1%	
Бег Б	(377)	-0 /0	(133)	+670	(118)	⊤0.170	(77)	+1070	(128)	-11/0	(138)	-1 /0	(4)
Det C	9125	+20%	8126	+7% 9124	+20%	8339	+10%	8124	+7%	7455	-1%		
	(522)	+20%	(132)	+ / 70	(147)	+20%	(87)	+1070	(156)	+ / 70	(138)	-1 %	

Among the three methods, the Integral Counting method produces the smallest relative difference from the static reactivity.

4.2 Case 2: Dropping SOR 3 and 4

In Case 2, both $\rho_{dyn,r}$ and $\rho_{dyn,c}$ were obtained from a single run of the McCARD/G TDMC calculation.

 $ho_{dyn,r}$ shows large R.Diff from ho_{st} , particularly when using the Extrapolation and Inverse method, which again highlights the limitation of relying on uncorrected raw data.

In contrast, $\rho_{dyn,c}$ calculated with the normalized amplitude function $\overline{p(t)}$ exhibits better agreement with the static reactivity. Across all three methods, the differences between $\rho_{dyn,c}$ and ρ_{st} are consistently reduced compared to those of $\rho_{dyn,r}$. As in Case 1, the Integral Counting method yields the smallest relative difference.

4. Conclusions

This study applied the modified rod drop experimental technique to the HANARO reactor to evaluate reactivity worth under two representative shut-off rod drop process.

Dynamic reactivity obtained directly from the measured number density showed noticeable deviations from the reference static reactivity. In contrast, when the normalized amplitude function was employed, the calculated dynamic reactivity exhibited better agreement with the static reactivity.

Among the several approaches, the Integral Counting method yielded the closest consistency with the static reactivity. Furthermore, the detector signal correction not only reduced the difference between dynamic and static reactivity, but yielded consistent results across different detectors within each method.

REFERENCES

- [1] W.C.Wang et al., The first application of large reactivity measurement through rod drop based on three-dimensional space-time dynamics, NUCL SCI TECH (2021) 32:13.
- [2] E. K. Lee, H. C. Shin, S. M. Bae et al., Application of the dynamic control rod reactivity measurement method to Korea Standard Nuclear Power Plants. In: Proceedings of the PHYSOR 2004, Chicago, IL, April 25-29(2004), ANS
- [3] S. M. Park, H. C. Lee, "Uncertainty Analysis for Graphite Isotope Ratio Method (GIRM) in a HANARO Simulation, Transactions of the Korean Nuclear Society Spring Meeting, 2024.
- [4] H. I. Kim, H. R. Kim, K. H. Lee and J. B. Lee (1996), "Design Characteristics and Startup Test of HANARO", Journal of nuclear Science and Technology, 33:7, 527-538, DOI: 10.1080/18811248.1996.9731952.
- [5] Shim, H. J., Han, B. S., Jung, J. S., Park, H. J., & Kim, C. H. (2012). McCARD: Monte Carlo code for advanced reactor design and analysis. Nuclear Engineering and Technology, 44(2), 161-176.
- [6] Ko, W. K., Jeong, S. J., Kim, Y. I. and Shim, H. J.(2024). Development of a GPU-enhanced time-dependent Monte Carlo neutron transport version of McCARD. EPJ Nuclear Sciences & Technologies, 10,28.
- [7] T. Misawa, H. Unesaki, C. H. Pyeon, Nuclear reactor physics experiments, Kyoto University, Kyoto, 2010.
- [8] J. J. Duderstadt, L. J. Hamilton, Nuclear reactor analysis, Wiley, New York, 1976.
- [9] J. M. Park, C. H. Pyeon, H. J. Shim, Sensitivity of a control rod worth estimate to neutron detector position by time-dependent Monte Carlo simulations of the rod drop experiment, Nucl. Eng. Technol. 56, 916 (2024).
- [10] K. O. Ott, R. J. Neuhold, Introductory Nuclear Reactor Dynamics, American Nuclear Society, Illinois, 1985.

Transactions of the Korean Nuclear Society Autumn Meeting Changwon, Korea, October 30-31, 2025

[11] H. J. Shim, D.H. Kim, M. Yamanaka, C. H. Pyeon, Estimation of kinetics parameters by Monte Carlo fixed-source calculations for point kinetic analysis of accelerator-driven system, Journal of Nuclear Science and Technology, 2020, VOL. 57, NO. 2, 177-186.